

# Some Modern Aspects of Self-Focusing Theory

Gadi Fibich

School of Mathematical Sciences, Tel Aviv University, Tel Aviv, Israel, fibich@tau.ac.il

**Summary.** In this Chapter, we give a brief summary of the “present status” of self-focusing theory, while trying to highlight the fascinating evolution of this theory.

## 1 Introduction

During the 1960s and early 1970s, there has been an intense theoretical and experimental research on self-focusing of intense laser beams in bulk media. In 1975, the results of this research activity were summarized in two long review papers: *Self focusing: Experimental*, by Shen [60], and *Self focusing: Theory*, by Marburger [50].

Around that time, mathematicians started to become interested in self focusing theory. A large part of this research effort concerned collapsing (i.e., singular) solutions of the 2D cubic Nonlinear Schrodinger equation (NLS)

$$i\psi_z(z, x, y) + \Delta\psi + |\psi|^2\psi = 0, \quad \Delta = \partial_{xx} + \partial_{yy}. \quad (1)$$

Here,  $\psi$  is the complex-valued electric field envelope,  $z$  is the direction of propagation, and  $x$  and  $y$  are the transverse coordinates. Let the Kerr medium be located at  $z > 0$ . Then, the NLS is solved for  $z > 0$ , subject to the initial condition

$$\psi(z = 0, x, y) = \psi_0(x, y), \quad -\infty < x, y < \infty,$$

where  $\psi_0$  is the envelope of the electric field that impinges on the Kerr medium interface at  $z = 0$ . Analysis of singular solutions of the NLS (1) turned out to be a hard mathematical problem for several reasons. First, the NLS is genuinely nonlinear, so linearization-based techniques are not applicable. Second, unlike the 1D cubic NLS, equation (1) is not integrable, so one cannot use inverse scattering theory. Finally, it turned out that the 2D cubic NLS is a “borderline case” for collapse in the following sense. Consider the  $d$ -dimensional focusing NLS with nonlinearity exponent  $p$ , i.e.,

$$i\psi_z(z, x_1, \dots, x_d) + \Delta\psi + |\psi|^{p-1}\psi = 0, \quad \Delta = \partial_{x_1x_1} + \dots + \partial_{x_dx_d}. \quad (2)$$

Then, the NLS (2) has collapsing solutions if  $(p - 1)d > 4$ , the *supercritical* case. When, however,  $(p - 1)d < 4$ , the *subcritical* case, there are no singular solutions.

Therefore,  $(p-1)d = 4$ , the *critical* NLS, is a “borderline case” for collapse. In particular, the NLS (1) for which  $p = 3$  and  $d = 2$  is critical. “As a result”, self-focusing in the NLS (1) is characterized by a delicate balance between the focusing Kerr non-linearity and diffraction. Hence, for example, collapse in the critical NLS is highly sensitive to small perturbations, which can arrest the collapse even when they are still small [31].

The present mathematical theory of self focusing is very different from the one in 1975, since it is mostly based on results that were obtained after 1975.<sup>1</sup> For various reasons, some of these results have not become part of the common knowledge of the nonlinear optics community. The goal of this Chapter is, thus, to provide a short survey of the current status of the mathematical theory of self focusing, and to express it in a nonlinear optics context. Obviously, we focus on the mathematical results which we believe are of most relevance to the nonlinear optics applications. For more extensive reviews, see [31, 62].

## 2 Some pre-1975 results

We begin with some pre-1975 results. The NLS (1) has several conservation laws. Of most importance are the conservation of *power*

$$P(z) \equiv P(0), \quad P(z) = \int |\psi|^2 dx dy,$$

and of the *Hamiltonian*

$$H(z) \equiv H(0), \quad H(z) = \int |\nabla\psi|^2 dx dy - \frac{1}{2} \int |\psi|^4 dx dy.$$

Another identity that plays an important role in NLS theory is the *variance identity* [65]. Let

$$V(z) = \int r^2 |\psi|^2 dx dy, \quad r = \sqrt{x^2 + y^2}.$$

Then,

$$\frac{d^2}{dz^2} V = 8H(0). \quad (3)$$

Since vanishing of variance can only occur if the whole solution collapses into the singularity, the variance identity leads to the following result:

**Theorem 1.** *Let  $\psi$  be a solution of the NLS (1) with initial condition  $\psi_0$ . Assume that one of the following three conditions holds:*

1.  $H(0) < 0$ .
2.  $H(0) = 0$  and  $\text{Im} \int \psi_0^*(x, y) \cdot \nabla \psi_0 dx dy < 0$ .

<sup>1</sup> The year 1975 was chosen as the ‘borderline’ between the ‘past’ and ‘present’ in self focusing theory, because of the review papers of Marburger and Shen [50, 60] that appeared in that year. Clearly, this choice is somewhat arbitrary.

$$3. H(0) > 0 \text{ and } \text{Im} \int \psi_0^*(x, y) \cdot \nabla \psi_0 dx dy \leq -\sqrt{H(0)V(0)},$$

where  $\nabla = (\partial_x, \partial_y)$  and  $\psi_0^*$  is the complex conjugate of  $\psi_0$ . Then,  $\psi$  becomes singular at a finite propagation distance.

An important symmetry of the critical NLS (1), known as the *lens transformation*, is as follows [63]. Let  $\psi$  be a solution of the NLS (1) with initial condition  $\psi_0(x, y)$ , and let  $\tilde{\psi}$  be the solution of the NLS (1) with initial condition  $\tilde{\psi}(0, x, y) = e^{-i\frac{r^2}{4F}} \psi_0(x, y)$ . Then,  $\tilde{\psi}$  is given by

$$\tilde{\psi}(z, x, y) = \frac{1}{L(z)} \psi(\zeta, \xi, \eta) e^{i\frac{Lz}{L} \frac{r^2}{4}},$$

where

$$L(z) = 1 - \frac{z}{F}, \quad \zeta = \int_0^z L^{-2}(s) ds, \quad \xi = \frac{x}{L}, \quad \eta = \frac{y}{L}.$$

## 2.1 Effect of a lens

Since

$$\frac{1}{z} = \frac{1}{F} + \frac{1}{\zeta}, \quad (4)$$

and since the addition of the quadratic phase term  $e^{-i\frac{r^2}{4F}}$  corresponds to adding a focusing lens with focal length  $F$  at  $z = 0$ , the lens transformation shows that in a bulk Kerr medium, the effect of a lens at  $z = 0$  is “the same” as in linear geometrical optics.

In particular, let  $Z_c$  be the collapse distance of a laser beam. If we now add a lens with focal length  $F$  at  $z = 0$ , then the new collapse distance, denoted by  $Z_c^F$ , follows immediately from equation (4), and is given by

$$\frac{1}{Z_c^F} = \frac{1}{F} + \frac{1}{Z_c}. \quad (5)$$

Therefore, the collapse distance decreases when the lens is focusing ( $F > 0$ ), increases when the lens is defocusing ( $F < 0$ ), and collapse is arrested by the defocusing lens if  $-Z_c < F < 0$ .

## 2.2 The $R$ (Townes) profile

The NLS (1) has waveguide solutions of the form  $\psi_{w-g} = e^{i\lambda^2 z} R_\lambda(r)$ , where  $R_\lambda(r) = \lambda R(\lambda r)$ , and  $R$  is the solution of

$$R''(r) + \frac{1}{r} R' - R + R^3 = 0, \quad R'(0) = 0, \quad R(\infty) = 0.$$

This equation turns out to have an infinite number of solutions. Of most interest, however, is the ground-state solution, known as the *R profile* or the *Townes profile*, which is positive and monotonically decreasing to zero.

The  $R$ -based waveguide solutions were originally considered by Chiao, Garmire and Townes [9] in the context of *self-trapping*, i.e., the observation of long and narrow filaments in experiments. It later turned out, however, that the NLS waveguide solutions  $\psi_{w-g}$  cannot be used to explain self-trapping, since they are unstable. Indeed, if we perturb the initial condition as  $\psi_0 = (1 + \epsilon)R(r)$ , where  $0 < \epsilon \ll 1$ , then the corresponding solution will collapse after a finite propagation distance [67]. Nevertheless, the  $R$  profile is extremely important in NLS theory, since it has the critical power for collapse (Section 3) and since it is the universal, self-similar profile of collapsing beams (Section 4).

### 3 Critical power

Kelley [41] was the first to predict that the key quantity that determines whether a beam would collapse is its input power (and not, e.g., its initial radius or focusing angle). During the sixties and seventies, however, there has been some confusion regarding the value of the critical power.

Weinstein [67] proved that a necessary condition for collapse is that the input power will exceed the power of the  $R$  profile, i.e., that  $P \geq P_{\text{cr}}$ , where

$$P_{\text{cr}} = \int R^2 dx dy \approx 11.70.$$

Merle [52, 53] proved that the only collapsing solutions with the *critical power*  $P = P_{\text{cr}}$  are those whose input profile is given by the  $R$  profile. Therefore, for any other input profile the threshold power for collapse  $P_{\text{th}}$  is strictly above  $P_{\text{cr}}$ . For example, the threshold power for a Gaussian profile  $\psi_0 = c \cdot \exp(-r^2)$  is  $\approx 2\%$  above  $P_{\text{cr}}$ , and for a super-Gaussian profile  $\psi_0 = c \cdot \exp(-r^4)$  is  $\approx 9\%$  above  $P_{\text{cr}}$  [21]. In general, the threshold power for collapse of an input profile which is “close” to the  $R$  profile will be lower (i.e., closer to  $P_{\text{cr}}$ ) than of an input profile which is “less similar” to the  $R$  profile.

Since the condition  $H(0) < 0$  implies collapse (see Section 2), some researchers estimated the threshold power for collapse from the condition of a zero Hamiltonian. Although  $P_{\text{cr}} = \int R^2 dx dy$  is only a *lower bound* for the threshold power, in the case of cylindrically-symmetric initial conditions, it provides a much better estimate for the threshold power than the one obtained from the condition of a zero Hamiltonian ([21], and see also Section 6.1).

The threshold power for collapse increases with input beam ellipticity. Fibich and Ilan [23] showed that for an elliptic input profile  $\psi_0 = cF(\sqrt{(x/a)^2 + (y/b)^2})$ , the threshold power for collapse can be approximated with

$$P_{\text{th}}(e) \approx \left[ 0.4 \frac{e + 1/e}{2} + 0.6 \right] P_{\text{th}}(e = 1),$$

where  $e = b/a$  and  $P_{\text{th}}(e = 1)$  is the threshold power for the circular profile  $\psi_0 = cF(r)$ . In this case, the threshold power obtained from the condition of a zero Hamiltonian is also highly inaccurate [23].

It is important to realize that while the threshold power  $P_{\text{th}}$  for collapse is above  $P_{\text{cr}}$ , the amount of power that eventually collapses into the blowup point is always equal to  $P_{\text{cr}}$  (see Section 6).

### 3.1 Hollow waveguides (bounded domains)

The propagation of laser beams in a hollow-core waveguide with radius  $r_a$  can be modeled by the NLS (1) on the bounded domain  $0 \leq x^2 + y^2 \leq r_a^2$ , subject to the boundary condition  $\psi(z, r = r_a) = 0$ . Fibich [18] proved that in this case,  $P_{\text{cr}}$  is still a *lower bound* for the threshold power. In addition, the numerical simulations of Fibich and Gaeta [21] suggest a stronger result, namely, that in this case the threshold power for collapse is *equal* to  $P_{\text{cr}}$  for “any” input profile. The reason for this behavior is that, unlike in bulk media, the reflecting walls prevent the shedding of power and keep the power localized in the transverse domain. Therefore, unlike in bulk medium, the collapsing core does not lose power due to radiation as it “re-arranges” itself in the form of the self-similar  $\psi_R$  profile (see Section 4).

## 4 The universal blowup profile $\psi_R$

The early analytical studies of collapsing solutions in the NLS (1) assumed that the blowup profile is a self-similar Gaussian or *sech* profile (see, e.g. [1]). Numerical simulations of collapsing NLS solutions that were carried out during the 1980s and early 1990s (see, e.g., [45]) showed, however, that regardless of the initial profile, near the singularity, collapsing NLS solutions approach the universal, self-similar profile  $\psi_R$ , which is a modulated  $R$  profile. In other words,  $\psi \sim \psi_R$  near the collapse point  $Z_c$ , where

$$|\psi_R| = \frac{1}{L(z)} R\left(\frac{r}{L(z)}\right),$$

and  $\lim_{z \rightarrow Z_c} L(z) = 0$ . Therefore, in particular, even if the initial condition is elliptically-shaped and/or noisy, near the singularity the blowup profile becomes smooth and symmetric.

The fact that collapsing NLS solutions approach the universal blowup profile  $\psi_R$  was crucial for the derivation of the reduced system (7) that was used to find the NLS blowup rate (see Section 7), as well as for the development of *modulation theory* for the asymptotic analysis of the effect of small perturbations (see Section 10.2). *Proving* the convergence to  $\psi_R$ , however, turned out to be a very hard mathematical problem. Indeed, this result was proved by Merle and Raphael [54] only in 2003, and its proof required developing new analytical tools. The proof of Merle and Raphael is valid for any initial condition whose power  $P$  satisfies  $P_{\text{cr}} < P < P_{\text{cr}} + \alpha$ , where  $\alpha$  is a universal constant whose value is less than  $P_{\text{cr}}$ . In particular, the proof holds for initial conditions which are elliptically-shaped or randomly distorted.

In 2003, Moll, Gaeta and Fibich [55] showed experimentally that the spatial profile of a collapsing beam evolves to the cylindrically-symmetric Townes profile, for elliptically-shaped, as well as for randomly distorted Gaussian input beams that propagated

in glass. Subsequently, in 2006, Grow et al. [40] observed experimentally the evolution to the Townes profile for collapsing Gaussian input pulses that propagated in water.

#### 4.1 New blowup profiles

Although the proof of Merle and Raphael does not hold for solutions whose power is above  $2P_{cr}$ , it was widely believed, based on numerous numerical simulations since the late 1970s, that any singular solution of the NLS collapses with the  $\psi_R$  profile. Even when the solution broke into multiple filaments (see Section 9), each filament was found to collapse with the  $\psi_R$  profile.

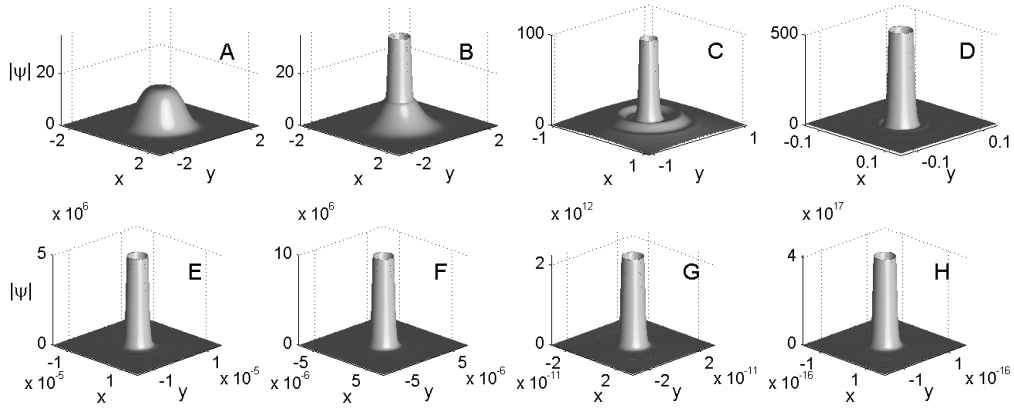


**Fig. 1.** Collapsing self-similar ring solution of the NLS (6) with  $\psi_0 = 15e^{-r^4}$ . From Ref. [22].

Recently, however, Fibich, Gavish and Wang [22] showed that high-power super-Gaussian beams collapse with a self-similar *ring profile*, which is different from the  $R$  profile, see Figure 1. Similarly to the  $\psi_R$  profile, these solutions are stable under radial perturbations. Therefore, the radially-symmetric NLS

$$i\psi_z(z, r) + \psi_{rr} + \frac{1}{r}\psi_r + |\psi|^2\psi = 0, \quad (6)$$

does have stable collapsing solutions whose blowup profile is not given by  $\psi_R$ . Unlike the  $\psi_R$  profile, however, these ring solutions are unstable under azimuthal perturbations. Therefore, the ring solutions are unstable as solutions of the NLS (1).

## 5 Super-Gaussian input beams

The self-focusing dynamics of super-Gaussian input beams is very different from the one of Gaussian beams. Here we briefly discuss some aspects of this topic. For more information and references, see the Chapter by Lukishova et al.

In the linear regime (i.e., for beam power  $\ll P_{\text{cr}}$ ), super-Gaussian evolve into a ring shape. This linear effect is due to Fresnel diffraction, and it occurs at propagation distances of the order of the diffraction (Fresnel) length, which is defined as  $L_{\text{diff}} = k_0 r_0^2$ , where  $k_0$  is the wavenumber and  $r_0$  is the input beam width. For high peak-power Nd:glass lasers, it was shown, both experimentally and numerically, that super-Gaussian profiles evolve into a ring profile [11, 43].

Grow et al. [40] showed theoretically that *ring formation of high-power super-Gaussian beams is a nonlinear phenomena which is due to ray bending as a result of nonlinear self-phase modulations* (see Figure 2). Therefore, ring formation of high-power super-Gaussian beams is a nonlinear geometrical optics effect, rather than a linear Fresnel diffraction one. This implies that it can occur over distances much shorter than a single diffraction length, and that this phenomena occurs for any  $N > 2$  in the initial profile  $\psi_0 = c \cdot \exp(-r^N)$  (see Figure 2).

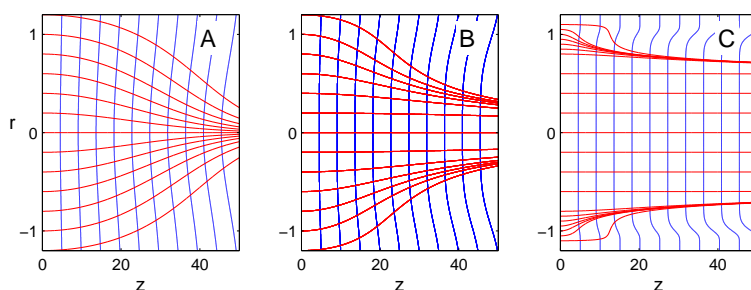


**Fig. 2.** Nonlinear propagation of rays (horizontal lines) and phase fronts (vertical lines) for high-power beams  $\psi_0 = c \cdot \exp(-r^N)$ . (A) Gaussian  $N = 2$ , (B) super-Gaussian  $N = 4$ , and (C) super-Gaussian  $N = 20$ . Graphs (A) and (B) are from Ref. [40].

In the absence of azimuthal noise, high-power super-Gaussian beams collapse with the self-similar ring profile described in Section 4.1 (see, e.g., Figure 1). These collapsing rings are, however, highly unstable under azimuthal perturbations. As a result, the ring quickly disintegrates into a ring of filaments, each of which collapses with the  $\psi_R$  profile.

In [40], both the ring formation and its subsequent propagation dynamics as it breaks up into a ring of filaments were observed experimentally for high-power super-Gaussian beams propagating in water. The diffraction length in these experiments was approximately 40cm, and the distances at which the rings were observed were usually less than 10cm. Therefore, the experimental data agrees with the ring developing at a fraction of a diffraction length. Figure 3 shows data from the same set of experiments that clearly shows the ring formation at high powers and its absence at low powers. This further confirms that ring formation for high-power super-Gaussian beams is a nonlinear phenomena.

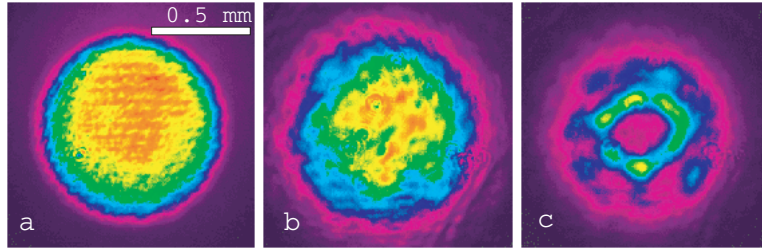


**Fig. 3.** Experimental intensity distributions for: (a) input profile, (b) linear output (low power) after a 7-cm cell, and (c) nonlinear output with  $E = 12.2 \mu\text{J}$  after a 7-cm cell. Data supplied by T.D. Grow and A.L. Gaeta.

Finally, we note that the collapse dynamics of high-power super-Gaussians implies that they can undergo multiple filamentation during the initial collapse at much lower powers ( $P \sim 10P_{\text{cr}}$ ) than Gaussian beams (see Section 9) [4, 40].

## 6 Partial beam collapse

The fact that the blowup profile is given by  $\psi_R$  implies that

$$|\psi|^2 \longrightarrow P_{\text{cr}} \cdot \delta(r), \quad z \rightarrow Z_c.$$

In other words, the amount of power that collapses into the singularity is independent of the initial condition, and is always given by  $P_{\text{cr}}$ .<sup>2</sup> We already saw that for any input profile different from the  $R$  profile, collapse can occur only if  $P > P_{\text{cr}}$ . Therefore, the “outer part” of the beam, whose power is equal to  $P - P_{\text{cr}}$ , does not collapse into the singularity, but rather continues to propagate forward. This shows that generically, only part of the beam power collapses into the singularity (*partial beam collapse*). Hence, *the variance at the collapse point is generically positive and not zero*, i.e.,

$$\lim_{z \rightarrow Z_c} V(z) > 0,$$

as was proved in 1989 by Nawa and Tsutsumi [56].

### 6.1 Common misinterpretations of the variance identity

There are some common *misinterpretations* of the variance identity, all of which follow from the wrong assumption that the variance vanishes at the blowup point: 1) The variance identity can be used to predict the collapse distance. 2) The threshold power can be well approximated from the condition of a zero Hamiltonian, 3) Solutions with positive Hamiltonian undergo partial-beam collapse whereas those with negative Hamiltonian undergo *whole-beam collapse* (i.e. all the beam power collapses into the focal point), etc. We stress that all of these statements are false, as they are based on the wrong assumption that the variance vanishes at the blowup point. See [23] for more details.

<sup>2</sup> This explains why in experiments it is often found that all filaments have the same power.

## 7 Blowup rate

In the rigorous mathematical theory of the NLS, the blowup rate is usually defined as  $L(z) = (\int |\nabla\psi|^2 dx dy)^{-1/2}$ . However, up to a multiplicative constant, the blowup rate can be defined as  $L = 1/\max_{x,y} |\psi(z, x, y)|$ . A question which has been open for many years is what is the blowup rate of NLS solutions. In other words, does  $L(z) \sim c(Z_c - z)^p$  for some  $p$  as  $z \rightarrow Z_c$ ?

### 7.1 The loglog law

Finding the blowup rate of the NLS turned out to be a very hard problem, and over the years various power-law relations were proposed [48]. In retrospect, the mathematical difficulties had to do with the fact that collapse in the *critical* NLS is “only” *quasi self-similar*, i.e., the collapsing core approaches the self-similar profile  $\psi_R$ , but the “outer part” of the beam has a completely different dynamics. Moreover, the coupling between these two components of the solution is exponentially weak. Eventually, Fraiman [37], and independently (and in a different way) Landman, LeMesurier, Papanicolaou, Sulem and Sulem [44, 46] showed that the NLS dynamics can be approximated with the following reduced ODE system for  $L(z)$ :

$$L_{zz}(z) = -\frac{\beta}{L^3}, \quad \beta_z(z) = -\frac{\nu(\beta)}{L^2}, \quad (7)$$

where  $0 < \beta \ll 1$ ,

$$\nu(\beta) = c_\nu e^{-\pi/\sqrt{\beta}}, \quad c_\nu = \frac{2A_R^2}{M}, \quad (8)$$

$A_R = \lim_{r \rightarrow \infty} e^r r^{1/2} R(r) \approx 3.52$ , and  $M = \frac{1}{4} \int_0^\infty r^2 R^2 r dr \approx 0.55$ . Asymptotic analysis of the reduced equations (7) showed that the blowup rate of the critical NLS is a square root with a loglog correction (the *loglog law*) [37, 44, 46]

$$L \sim \left( \frac{2\pi(Z_c - z)}{\ln \ln(1/(Z_c - z))} \right)^{1/2}, \quad z \rightarrow Z_c. \quad (9)$$

Subsequent numerical simulations with specialized codes that could reach very high focusing levels (e.g.,  $1/L = O(10^{10})$ ) have confirmed that the blowup rate is slightly faster than a square root, but failed to detect the loglog correction. The reason for this “failure” was explained by Fibich and Papanicolaou [16, 31], who showed that the loglog law does not become valid even after the solution has focused by  $10^{100}$ . Since the validity of the NLS model breaks down at much lower focusing levels, the loglog law turned out to be more of mathematical interest than of real physical value. However, Malkin [49] and Fibich [16] showed that the same reduced equations that lead to the loglog law, equations (7), can be solved differently, yielding the *adiabatic laws of collapse*, which become valid after moderate focusing levels [31]. More importantly, Fibich and Papanicolaou [31] showed that a similar approach can be used to analyze the effect of small perturbations on the collapse dynamics at physically-relevant focusing levels (see Section 10.2).

Although the loglog law (9) was derived in the late 1980s, a rigorous proof was obtained only in 2003 by Merle and Raphael [54]. The proof holds for all initial conditions whose power  $P$  satisfies  $P_{\text{cr}} < P < P_{\text{cr}} + \alpha$ , where  $\alpha$  is a universal constant which is smaller than  $P_{\text{cr}}$ .

## 7.2 A square-root law

Although the rigorous proof of Merle and Raphael does not hold for input powers  $P > 2P_{\text{cr}}$ , it was widely believed that generically, all NLS solutions collapse according to the loglog law. However, in 2005, Fibich, Gavish and Wang showed asymptotically and numerically that collapsing self-similar *ring* solutions of the NLS (see, e.g., Figure 1) blowup at a square-root rate, with no loglog correction [22]. At present, it is still an open question whether the self-similar ring profile, hence the square-root blowup rate, is maintained all the way up to the singularity. Indeed, the numerical simulations of [22] become unreliable after focusing by  $\approx 10^{16}$ . Therefore, it is possible that at higher focusing levels the self-similar ring profile would change to the Townes profile, in which case the blowup rate would change from a square root to the loglog law. This open question is, however, only of mathematical interest, as the validity of the NLS model breaks down at much smaller focusing levels.

## 8 Self-focusing distance

It would have been very useful to have an exact analytical formula for the location of the singularity as a function of the input beam. Unfortunately, such a formula does not exist. Some researchers estimated the location of the blowup point by using the variance identity (3) to calculate the location where the variance should vanish. As we pointed out in Section 6.1, this approach usually leads to very inaccurate results. Fibich [16] used the *adiabatic law of collapse* to derive the following asymptotic formula for real initial conditions (i.e. for collimated beams)

$$Z_c \sim \sqrt{\frac{MP_{\text{cr}}}{P/P_{\text{cr}} - 1}} \left( \int |\nabla\psi_0|^2 \right)^{-1}, \quad (10)$$

which gives reasonable predictions for  $P \leq 2P_{\text{cr}}$ .

In the absence of an analytical formula, the only way to find the location of the singularity is through numerical simulations. For example, Dawes and Marburger [12] used the results of numerical simulations to derive the following *curve-fitted* formula for the location of the singularity of collimated *Gaussian* input beams  $\psi_0 = ce^{-r^2/2}$ :

$$Z_c = 0.367[(\sqrt{P/P_{\text{cr}}} - 0.852)^2 - 0.0219]^{-1/2}. \quad (11)$$

Kelley [41] was the first to show that the collapse distance  $Z_c$  scales as  $1/\sqrt{P}$  for  $P \gg P_{\text{cr}}$ . In theory, the  $1/\sqrt{P}$  relation should become more and more accurate as  $P$  increases. This is, indeed, the case when the input beam is noiseless. In practice, however, input beams are always noisy. At input powers that are roughly above

$100P_{cr}$ , the propagation becomes highly sensitive to the effect of input beam noise. As a result, the beam becomes modulationally unstable and breaks into multiple filaments at a distance that scales as  $\sim 1/P$ . Campillo, Shapiro and Suydam [6] predicted theoretically, and observed experimentally for continuous-wave (cw) beams propagating in  $CS_2$ , that this noise-induced multiple filamentation implies that the collapse distance scales as  $1/P$ . This result was rediscovered by Fibich et al. [19], who also observed numerically, and experimentally for femtosecond pulses propagating in air, that the collapse distance scales as  $1/\sqrt{P}$  for input powers that are moderately above the critical power for self focusing, but that at higher powers the collapse distance scales as  $1/P$ .

### 8.1 Effect of a lens

Let  $Z_c$  be the collapse distance of a laser beam. As we have seen before, if we add a lens with focal length  $F$  at  $z = 0$ , then the new collapse distance, denoted by  $Z_c^F$ , is given by equation (5). Using this lens relation, one can predict the collapse point of focused beams based on predictions for the collapse point of collimated beams, such as equation (10) or (11).

Recently, Fibich et al. [34] showed that this lens relation is in excellent agreement with experimental measurements of the collapse distance in atmospheric propagation of femtosecond pulses. This showed that the relatively simple NLS model (1) can be used to predict the collapse point, since all other mechanisms (multiphoton absorption, plasma formation, Raman scattering, etc.) become important only *after* the pulse has collapsed.

## 9 Multiple filamentation

Since the early 1960s, it was observed experimentally that when the laser power is significantly larger than the critical power  $P_{cr}$ , the beam can break into several long and narrow filaments, a phenomenon known as *multiple filamentation* (MF) or as *small-scale self-focusing*. Since MF involves a complete breakup of the beam cylindrical symmetry, it must be initiated by a symmetry-breaking mechanism.

### 9.1 Noise-induced multiple filamentation

For many years, the standard (and only) explanation for MF in the literature, due to Bespalov and Talanov [5], has been that it is initiated by input beam noise. Briefly, the noise leads to a *modulational instability* (MI), which ultimately results in MF. Although the analysis of Bespalov and Talanov was based on linear stability of (infinite power) plane waves solutions of the NLS (1), it was believed to hold for beams whose power is roughly above  $10P_{cr}$ . This is, however, not the case. For example, Fibich and Ilan [24] solved numerically the NLS (1) with an input Gaussian beam with  $P = 15P_{cr}$  and 10% random noise, and observed that it did not break into multiple filaments, but rather collapsed at a single location. Indeed, noise would lead to MF of Gaussian

beams the NLS (1) only when the distance for noise-induced MF,  $L_{\text{MF}}$ , is smaller than the self-focusing distance  $Z_c$ . Since  $L_{\text{MF}} \sim 1/P$  and  $Z_c \sim 1/\sqrt{P}$ , this would occur for powers above a second power threshold  $P_{\text{th}}^{(2)}$ , which is roughly of the order of  $100P_{\text{cr}}$ . Therefore, input beam noise would lead to MF in the NLS (1) only for  $P > P_{\text{th}}^{(2)}$  [6, 19].

Until recently, the only known way to observe noise-induced MF numerically at input powers  $\ll P_{\text{th}}^{(2)}$  was to add to the NLS a collapse-arresting mechanism. Consider, for example, the 2D NLS with a nonlinear saturation

$$i\psi_z(z, x, y) + \Delta\psi + \frac{|\psi|^2}{1 + \epsilon|\psi|^2}\psi = 0, \quad \epsilon > 0, \quad \Delta = \partial_{xx} + \partial_{yy}. \quad (12)$$

Solutions of this equation do not become singular. Rather, when the input power is above  $P_{\text{cr}}$ , the solution initially self-focuses, but then the collapse is arrested (see Figures 4–5). Subsequently, the solution undergoes focusing-defocusing cycles (a *multifocus structure*). During the defocusing stage of each cycle, the solution has a ring (or crater) shape. Since a ring is an unstable shape for a beam, it can disintegrate into multiple filaments in the presence of noise, as was first demonstrated numerically in 1979 by Konno and Suzuki [42]. Soto-Crespo, Wright and Akhmediev [61] developed an approximate stability analysis that explains the instability of the rings and predicts the number of filaments.

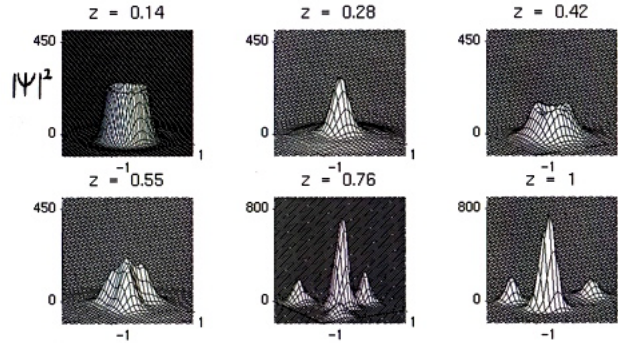


**Fig. 4.** Solution of equation (12) with a noisy input Gaussian beam with power  $P \approx 15P_{\text{cr}}$ . From Ref. [24].

It is important to note that the two ingredients needed for MF at input powers  $\ll P_{\text{th}}^{(2)}$  are:

1. A “mechanism” that arrests the collapse, so that as the beam defocuses it will assume the unstable ring shape. This mechanism does not have to be nonlinear saturation. For example, in [27] the collapse-arresting mechanisms were nonparaxiality and vectorial effects.

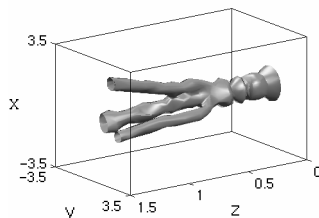


**Fig. 5.** Iso-intensity surface of the solution of Fig. 4. Note that the beam propagates from right to left. From Ref. [24].

Recently, it turned out that this mechanism does not even have to be collapse-arresting, as the only real requirement is that it will make the beam assume the unstable ring shape. Moreover, the ring does not have to be defocusing, since a collapsing ring is also unstable. Indeed, this is the case in MF of high-power Super-Gaussian beams [40], where the ring is formed as the beam is collapsing (see Section 4.1), and also in MF of collapsing vortices [66].

2. A “mechanism” that breaks the symmetry of the ring. This can be input-beam noise, but also deterministic input-beam astigmatism [26, 27, 39] or vectorial effects [24, 25] (see Section 9.2).

There are several important differences between noise-induced multiple filamentation for  $P \ll P_{\text{th}}^{(2)}$  and for  $P \geq P_{\text{th}}^{(2)}$  [19]. When  $P \ll P_{\text{th}}^{(2)}$ , the beam initially collapses as a single filament, then undergoes a few focusing-defocusing cycles and only then breaks into MF (see, e.g., Figure 5). In this case, the distance where MF occurs scales as  $1/\sqrt{P}$ . When, however,  $P \geq P_{\text{th}}^{(2)}$ , MF occurs during the initial collapse, and the distance where MF occurs scales as  $1/P$ . Indeed, in the experiments in [19], it was observed that the beam initially collapses as a single filament in the  $1/\sqrt{P}$  “low-power” regime, but as multiple filaments in the  $1/P$  “high-power” regime.

## 9.2 Deterministic multiple filamentation

Since noise is by definition random, the MF pattern of noise-induced MF would be different from shot to shot; i.e., the number and location of the filaments is unpredictable. This constitutes a serious drawback in applications in which precise localization is crucial.

Recall that the NLS is only the leading-order model for propagation of linearly-polarized beams in a Kerr medium, and that a more comprehensive model is given by the vectorial Helmholtz equations. In the latter model, a linear polarization state breaks up the cylindrical symmetry by inducing a preferred direction, which is the direction of the linear polarization state. Fibich and Ilan [24, 25] showed numerically that the deterministic breakup of cylindrical symmetry by a linear polarization state can lead to a deterministic multiple filamentation. However, vectorial-effects induced MF has not been observed in experiments [14]. The reason for this is probably as follows. In order that the vectorial coupling between the electric fields component would lead to

MF, the beam radius should self-focus down to approximately two wavelengths. In experiments, however, self-focusing is arrested at a much earlier stage, due to plasma effects.

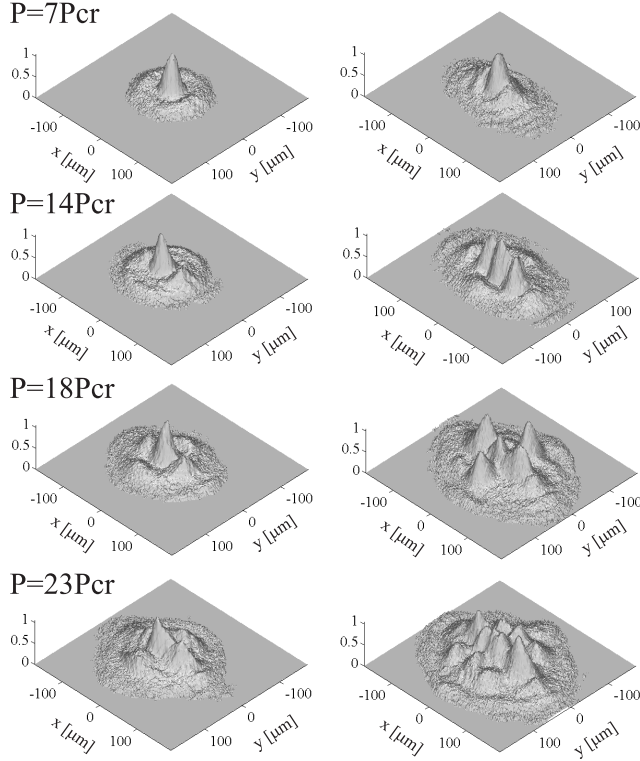


**Fig. 6.** Normalized 3D views of filamentation patterns after propagation of 31mm in water, for a near-circular incident beam ( $e=b/a = 1.09$ , left panel) and elliptical incident beam ( $e=2.2$ , right panel). The major axis of the ellipse lies along the  $x$ -axis of the plots. From Ref. [14].

In [26, 27, 39] it was predicted theoretically and observed for laser pulses propagating in sodium vapor [39] and in water [14] that input beam astigmatism can also lead to a deterministic MF pattern, i.e., a pattern that is reproducible from shot to shot. Dubietis et al. [14] pointed out that when the input beam is elliptically-shaped, e.g.,  $\psi_0 = c \cdot \exp(-(x/a)^2 - (y/b)^2)$ , the MF pattern can only consist of a combination of (1) a single on-axis central filament, (2) pairs of identical filaments located along the ellipse major axis at  $(\pm x, 0)$ , pairs of identical filaments located along the minor axis at  $(0, \pm y)$ , and (4) quadruples of identical filaments located at  $(\pm x, \pm y)$ . Moreover, in that study all the above four filament types were observed experimentally in water (see Figure 6) and numerically. Subsequent approaches for deterministic MF which is induced by a deterministic breakup of the input beam symmetry include a tilted lens and a phase mask [20, 51]. In [20], it was shown experimentally that sufficiently large

astigmatism can dominate noise in the determination of the MF pattern in atmospheric propagation. Hence, rather than trying to eliminate noise, one can control the MF pattern by adding sufficiently large astigmatism.

## 10 Perturbation theory: Effect of small mechanisms neglected in the NLS model

The 2D cubic NLS (1) is the leading-order model for propagation of intense laser beams in a Kerr medium. As we have seen, in the NLS model the electric field intensity becomes infinite at the blowup point. Since physical quantities do not become infinite, this indicates that near the blowup point, some physical mechanisms that were neglected in the derivation of the NLS become important. Moreover, since the NLS (1) is *critical* (see Section 1), these mechanisms can have a large effect even when they are still small compared with the Kerr nonlinearity or diffraction.

### 10.1 Unreliability of aberrationless approximation and variational methods

Since a direct analysis of NLS equations with additional perturbations is hard, the standard approach has been to approximate these equations with reduced equations that do not depend on the transverse  $(x, y)$  coordinates, and then to analyze the (much simpler) reduced equations. The key issue, naturally, has been how to derive the “correct” reduced equations.

Starting with [1], for many years all the derivations used the *aberrationless approximation*, i.e., the assumption that during its propagation, the beam maintains a known self-similar profile

$$|\psi| \sim \frac{1}{L(z)} G\left(\frac{r}{L(z)}\right),$$

where  $G$  is a Gaussian, *sech*, etc. In the *aberrationless approximation method*, this self-similar profile is substituted in the NLS, and the reduced equations follow from balancing the leading-order terms. In the *variational method*, the self-similar profile is substituted in the NLS Lagrangian. Integration over the  $(x, y)$  coordinates gives the averaged Lagrangian, whose variational derivative gives the reduced equations.

There has been a considerable research effort on the optimal way to derive the reduced equations using either of these two methods. However, as was pointed out and explained in [23], both methods are unreliable, in the sense that they sometimes lead to predictions that are quantitatively inaccurate, or even qualitatively wrong. It is important to note that the unreliability of the aberrationless approximation and variational methods is related to the fact that the NLS (1) is *critical*. Indeed, these methods have been successful in analysis of perturbed non-critical NLS, such as the perturbed one-dimensional cubic NLS.

The reason for the unreliability of these methods is that they make use of the *aberrationless approximation*. One problem with this approximation is that it implicitly implies that when collapse occurs, all the beam collapses into the focal point (*whole*

*beam collapse*), whereas, in fact, collapsing beams undergo *partial beam collapse* (see Section 6). Another problem with this approximation is that it has been usually applied with the wrong profile, i.e., with a profile  $G$  different from the  $R$  profile. This may not seem like a serious issue, as a well-fitted Gaussian can be quite close to the  $R$  profile. However, the  $R$  profile is the *only* profile that has 1) the critical power for collapse, and 2) a zero Hamiltonian. Hence, it is a borderline case for the two conditions for collapse  $P > P_{cr}$  and  $H < 0$ . These two properties are at the heart of the sensitivity of the  $\psi_R$  profile to small perturbations, which cannot be captured by any self-similar profile which is not based on the  $R$  profile.

It may seem, therefore, that one can use the aberrationless approximation, so long that it is being used with the  $\psi_R$  profile. Even this is not true, however, since the  $\psi_R$  profile represents a complete balance between diffraction and nonlinearity. Hence, the collapse dynamics is determined by the *small difference* between  $\psi$  and  $\psi_R$ . Therefore, the derivation of the reduced equations should be based on balancing the leading-order deviations from  $\psi_R$ .

## 10.2 Modulation theory

As noted, in order to derive the “correct” reduced equations, one should take into account that

1. As the solution collapses, its profile approaches the  $\psi_R$  profile.
2. The collapse dynamics is determined by the *small differences* from  $\psi_R$ .

Fibich and Papanicolaou [31] used these observations to derive a systematic method for deriving reduced equations for the effect of additional small mechanisms on critical self-focusing, known as *modulation theory*.<sup>3</sup> Consider the NLS with a general small perturbation  $\epsilon F$

$$i\psi_z(z, x, y) + \Delta\psi + |\psi|^2\psi + \epsilon F(\psi) = 0, \quad \Delta = \partial_{xx} + \partial_{yy}. \quad (13)$$

As the solution collapses, its profile becomes closer to  $\psi_R$ . Once that happens, self focusing in the perturbed NLS (13) is given, to leading order, by the reduced ODE system

$$\beta_z(z) + \frac{\nu(\beta)}{L^2} = \frac{\epsilon}{2M}(f_1)_z - \frac{2\epsilon}{M}f_2, \quad L_{zz}(z) = -\frac{\beta}{L^3}, \quad (14)$$

where

$$f_1(z) = 2L(z) \cdot \text{Re} \int F(\psi_R) e^{-iS} [R(\rho) + \rho R'(\rho)] dx dy, \quad (15)$$

$$f_2(z) = \text{Im} \int F(\psi_R) \psi_R^* dx dy, \quad (16)$$

and

---

<sup>3</sup> Not to be confused with modulational instability, which refers to the destabilizing effect of small perturbations in the input profile, see Section 9.1.

$$S(z, r) = \zeta(z) + \frac{L_z}{L} \frac{r^2}{4}, \quad \rho = \frac{r}{L}, \quad \zeta = \int_0^2 L^{-2}(s) ds.$$

As expected, when  $\epsilon = 0$ , equations (14) become the reduced equations (7) for the unperturbed NLS. The effect of the perturbation enters through the auxiliary functions  $f_1$  and  $f_2$ , which correspond to the conservative and nonconservative components of the perturbation, respectively.

The reduced equations (14) have been used to analyze the effect of various small perturbations, such as a weak defocusing quintic nonlinearity, saturating nonlinearities, small normal time dispersion, nonparaxiality, vectorial effects, linear and nonlinear damping and Debye relaxation [30, 17, 32, 49, 18, 24, 27]. In all cases, the predictions of the reduced equations were found to be in full agreement with numerical simulations of the corresponding perturbed NLS.

The reduced equations (14) show that additional mechanisms can have a large effect on the self-focusing dynamics even when they are still small compared with the Kerr nonlinearity and diffraction. This ‘sensitivity’ property is unique to the *critical* NLS (see Section 1), and it reflects the fact that in critical collapse, the Kerr nonlinearity is nearly balanced by diffraction. Hence, a small mechanism can shift the delicate balance between these two competing (much larger) effects, and even arrest the collapse [31].

## 11 Effect of normal group velocity dispersion

The basic model for propagation of *ultrashort pulses* in a bulk Kerr medium is given by the NLS with group velocity dispersion (GVD)

$$i\psi_z(z, x, y, t) + \Delta\psi - \gamma_2\psi_{tt} + |\psi|^2\psi = 0, \quad \Delta = \partial_{xx} + \partial_{yy}, \quad (17)$$

where

$$\gamma_2 = \frac{r_0^2 k_0 k_0''(\omega_0)}{T_0^2}$$

is the dimensionless GVD parameter, and  $r_0$ ,  $T_0$ ,  $k_0$  and  $\omega_0$  are the input pulse radius, temporal duration, wavenumber and carrier frequency, respectively.

When dispersion is *anomalous* ( $\gamma_2 < 0$ ) the pulse undergoes temporal and transverse compression. Indeed, in that case eq. (17) is the 3D [i.e.,  $(x, y, t)$ ] supercritical NLS (see Section 1), which has solutions that become singular in finite distance  $z$ . The dynamics in the case of *normal GVD* ( $\gamma_2 > 0$ ) is much more complicated, however, because of the opposite signs of diffraction and dispersion.

The question whether small normal dispersion can arrest singularity formation has defied research efforts for many years. In 1986, Zharova et al. [68] derived a reduced ODE for the evolution (in  $z$ ) of the pulse amplitude at  $t_m$ , the time of the initial peak amplitude. Analysis of this ODE showed that small normal GVD arrests the collapse at  $t_m$ . As a result, the pulse splits into two temporal peaks which continue to focus. The numerical simulations of Zharova et al. confirmed the predicted pulse splitting, and also showed what was interpreted as a secondary splitting. Therefore, Zharova et

al. conjectured that the new peaks would continue to split into “progressively smaller-scale”, and hence that small normal dispersion would arrest self-focusing through multiple splitting.

Numerical simulations of eq. (17) carried during the 1990s [47, 58, 7, 30, 57, 13] showed that self-focusing of the two peaks leads to the formation of temporal shocks at the peaks edges. As a result, in all the above studies, which used ‘standard’ numerical methods, the simulations could not go beyond the shock formation and were thus unable to determine whether secondary splittings occur and whether the solution ultimately becomes singular. In 1995, Fibich, Malkin and Papanicolaou [30] used *modulation theory* (see Section 10.2) to derive a reduced system of PDEs for self-focusing in (17) which is valid for all  $t$  cross-sections, and not just for  $t_m$ . Analysis of the reduced system showed that while self-focusing is arrested in the near vicinity of  $t_m$ , it continues elsewhere, i.e., that small normal GVD does not arrest the collapse. However, the validity of the reduced system breaks down as the shock edges of the two peaks form. Therefore, one cannot use the reduced system to predict whether multiple splitting would occur and/or whether the solution ultimately becomes singular. Analysis of the reduced system did reveal, however, that temporal splitting is associated with the transition from independent 2D collapse of each  $t$  cross-section to a full 3D dynamics. Therefore, it was suggested in [30] that the two peaks would not necessarily split again.

Temporal splitting of ultrashort pulses was first observed experimentally in 1996 by Ranka and Gaeta [57] and later by Diddams et al. [13]. In these experiments secondary splittings were also observed at even higher input powers. Nevertheless, these observations do not imply that solutions of eq. (17) undergo multiple splittings, because these secondary splittings were observed at such high powers where the validity of eq. (17) breaks down, as additional physical mechanisms become important.

In 2001, Germaschewski et al. [38] used an adaptive mesh refinement method to solve eq. (17) beyond the pulse splitting. These simulations show that after the pulse splitting the two peaks do not undergo a similar secondary splitting. Rather, the collapse of the two peaks is arrested by dispersion. Similar results were also obtained by Fibich, Ren and Wang using the iterative grid distribution method [33]. In that study, the authors solved eq. (17) with the same initial conditions used by Zharova et al. in [68] and observed no secondary splitting, thus confirming that the numerical observation of secondary splitting in that study was in fact a numerical artifact.

Based on the numerical simulations of [10, 33, 38], it is now believed that after the pulse splitting the two peaks do not undergo a secondary splitting, and that small normal GVD arrests the collapse of the two peaks. However, a rigorous proof that solutions of eq. (17) cannot become singular is still not available, and is considered a hard analytical problem.

## 12 Nonparaxiality and backscattering

In nonlinear optics, the NLS model is derived from the more comprehensive scalar nonlinear Helmholtz equation (NLH)

$$E_{xx}(x, y, z) + E_{yy} + E_{zz} + k_0^2 (1 + 4\epsilon_0 cn_2 |E|^2) E = 0. \quad (18)$$

In general,  $E = e^{ik_0z}\psi(z, x, y) + e^{-ik_0z}B(z, x, y)$ , where  $\psi$  and  $B$  are the slowly-varying envelopes of the forward-propagating and backscattered waves, respectively. The NLS is derived by *neglecting the backscattered wave* (i.e., setting  $B \equiv 0$ ) and then applying the *paraxial approximation*

$$\psi_{zz} \ll k_0\psi_z.$$

Since there are no singularities in nature, a natural question is whether initial conditions that lead to blowup in the NLS, correspond to global (i.e., non-singular) solutions of the corresponding NLH. In other words, do nonparaxiality and backscattering arrest the collapse, or is collapse arrested only in a more comprehensive model than the NLH (18).

The observation that the paraxial approximation breaks down near the singularity has already been noted in 1965 by Kelley in [41]. Vlasov [64] derived a perturbed NLS that includes the leading-order effect of nonparaxiality. He solved numerically this equation, and observed that collapse is arrested in this “nonparaxial NLS”. Feit and Fleck [15] used numerical simulations of the NLH to show that nonparaxiality can arrest the blowup for initial conditions that lead to singularity formation in the NLS (1). After the arrest of collapse in the NLH, the beam undergoes focusing-defocusing oscillations (*multiple foci*). In these simulations, however, they did not solve a true boundary value problem for the NLH. Instead, they solved an initial value problem for a “modified” NLH that describes only the forward-going wave (while introducing several additional assumptions along the way). Akhmediev and collaborators [3, 2] analyzed an initial-value problem for a different “modified” NLH; their numerical simulations also suggested that nonparaxiality arrests the singularity formation. All of the above numerical approaches ([64, 15, 3, 2]), however, did not account for the effect of backscattering. Fibich [17] used *modulation theory* (see Section 10.2) to derive a reduced ODE (in  $z$ ) for self-focusing in the presence of small nonparaxiality. His analysis suggests that nonparaxiality indeed arrests the singularity formation, resulting instead in decaying focusing-defocusing oscillations. Moreover, it showed that nonparaxiality arrests collapse while it is still small compared with the focusing Kerr nonlinearity. However, backscattering effects were neglected in this asymptotic analysis.

In [35, 36], Fibich and Tsynkov developed a novel numerical method for solving the NLH as a true boundary value problem. The key issue has been to develop a *two-way absorbing boundary condition* that allows for the impinging electric field to enter the Kerr medium, while allowing the backscattered wave to be fully transmitted in the opposite direction. This method allowed for the first quantitative calculation of backscattering due to the nonlinear Kerr effect [28]. Unfortunately, so far the method can only compute solutions whose input power is below  $P_{\text{cr}}$ , leaving open the issue of global existence of solutions with power above  $P_{\text{cr}}$  in the NLH model. Some progress in that direction was made in [29], when Fibich, Ilan and Tsynkov used the same numerical method to compute global solutions of the linearly-damped NLH for initial conditions that lead to collapse in the corresponding linearly-damped NLS. For these solutions, therefore, the arrest of collapse has to be due to nonparaxiality and backscattering. Recently, Sever proved that solutions of the NLH exist globally [59]. However,

Sever's proof holds only for real boundary conditions, whereas the correct physical radiation boundary conditions that allow for power propagation are complex-valued. Therefore, all the results so far suggest that nonparaxiality and backscattering arrest the collapse, but a rigorous proof of this result is still an open problem.

Finally, we note that the NLH (18) is derived under the assumption of linear polarization, and that a more comprehensive model is the vectorial NLH for the three components of the vector electrical field [8]. The effects of the coupling to the two other components of the electric field are of the same order as nonparaxiality, and have the same qualitative effect on the arrest of collapse, but are  $\approx 7$  times stronger [24].

### 13 Final remarks

At present, there is a fairly good understanding of self-focusing of “low power” beams, i.e., those whose power is moderately above the critical power  $P_{\text{cr}}$ . Indeed, since they collapse with the  $\psi_R$  profile, one can use *modulation theory* to analyze the effects of most perturbations. There are still some open mathematical questions, such as proving rigorously that normal dispersion or nonparaxiality arrest the collapse (Sections 11 and 12). However, the lack of rigorous proofs for these open problems is probably a “mathematical issue”, which “need not concern” the nonlinear optics community.

In recent years, there is a growing evidence that the self-focusing dynamics of “high power” beams, i.e., those whose power is many times the critical power  $P_{\text{cr}}$ , is very different from the one of “low power” beams. Indeed, “high power” beams can undergo multiple filamentation prior to the initial collapse (Section 9), have a different scaling law for the collapse distance (Section 8), and collapse with self-similar ring profile which is different from  $\psi_R$  (Section 4.1). At present, there is no good understanding of self focusing of “high power” beams, and most results are based either on numerical simulations or on elementary analysis. For example, there is no good theory for multiple filamentation that can predict the number of filaments of an input beam, whether two close filaments will merge into a single filaments, etc. The lack of a good theory for the “high power beams” is because, unlike “low power” beams, there is no universal attractor  $\psi_R$ . Developing new analytical tools for the “high power” regime is probably one of key challenges for the future of self-focusing theory.

### References

- S.A. Akhmanov, A.P. Sukhorukov and R.V. Khokhlov. Self-focusing and self-trapping of intense light beams in a nonlinear medium. *JET* **23**, 1025–1033 (1966)
- N. Akhmediev, A. Ankiewicz, and J.M. Soto-Crespo. Does the nonlinear Scharödinger equation correctly describe beam propagation? *Opt. Lett.* **18**, 411–413 (1993)
- N. Akhmediev and J.M. Soto-Crespo. Generation of a train of three-dimensional optical solitons in a self-focusing medium. *Phys. Rev. A* **47**, 1358–1364, (1993)
- L. Bergé, C. Goutéduard, J. Schjodt-Erikson and H. Ward. Filamentation patterns in Kerr media vs. beam shape robustness, nonlinear saturation and polarization states. *Physica D* **176**, 181-211, (2003)

- V.I. Bespalov and V.I. Talanov. Filamentary structure of light beams in nonlinear media. *Hiz. Eksper. Tenor. Fizz. - Pis'ma Redact. (U.Sis.R. JET)*, **3**, 471–476, 1966. Transf. in *JET Lett.* **3**, 307–310 (1966).
- A.J. Campillo, S.L. Shapiro, and B.R. Suydam. Relationship of self-focusing to spatial instability modes. *Apple. Phys. Lett.* **24**, 178–180 (1974)
- P. Chernev and V. Petrov. Self-focusing of light pulses in the presence of normal group-velocity dispersion. *Opt. Lett.* **17**, 172–174 (1992)
- S. Chi and Q. Guo. Vector Theory of Self-Focusing of an optical beam in Kerr media. *Opt. Lett.* **20**, 1598–1560 (1995)
- R.Y. Chiao, E. Garmire, and C.H. Townes. Self-trapping of optical beams. *Phys. Rev. Lett.* **13**, 479–482 (1964)
- J. Coleman and C. Sulem. Numerical simulations of blow-up solutions of the vector nonlinear Schrödinger equation. *Phys. Rev. E* **66**, 036701 (2002)
- V.R. Costich and B.C. Johnson. Apertures to shape high-power laser beams. *Laser Focus* **10**, 43–46 (1974)
- E.L. Dawes and J.H. Marburger. Computer studies in self-focusing. *Phys. Rev.* **179**, 862–868 (1969)
- S.A. Diddams, H.K. Eaton, A.A. Zozulya, and T.S. Clement. Amplitude and phase measurements of femtosecond pulse splitting in nonlinear dispersive media. *Opt. Lett.* **23**, 379–381 (1998)
- A. Dubietis, G. Tamošauskas, G. Fibich, and B. Ilan. Multiple filamentation induced by input-beam ellipticity. *Opt. Lett.* **29**, 1126–1128 (2004)
- M.D. Feit and J.A. Fleck. Beam nonparaxiality, filament formation, and beam breakup in the self-focusing of optical beams. *J. Opt. Soc. Am. B* **5**, 633–640 (1988)
- G. Fibich. An adiabatic law for self-focusing of optical beams. *Opt. Lett.* **21**, 1735–1737 (1996)
- G. Fibich. Small beam nonparaxiality arrests self-focusing of optical beams. *Phys. Rev. Lett.* **76**, 4356–4359 (1996)
- G. Fibich. Self-focusing in the damped nonlinear Schrödinger equation. *SIAM. J. Appl. Math* **61**, 1680–1705 (2001)
- G. Fibich, S. Eisenmann, B. Ilan, Y. Erlich, M. Fraenkel, Z. Henis, A.L. Gaeta, and A. Zigler. Self-focusing distance of very high power laser pulses. *Opt. Express* **13**, 5897–5903 (2005)
- G. Fibich, S. Eisenmann, B. Ilan, and A. Zigler. Control of multiple filamentation in air. *Opt. Lett.* **29**, 1772–1774 (2004)
- G. Fibich and A. Gaeta. Critical power for self-focusing in bulk media and in hollow waveguides. *Opt. Lett.* **25**, 335–337 (2000)
- G. Fibich, N. Gavish, and X.P. Wang. New singular solutions of the nonlinear Schrödinger equation. *Physica D* **211**, 193–220 (2005)
- G. Fibich and B. Ilan. Self focusing of elliptic beams: An example of the failure of the aberrationless approximation. *JOSA B* **17**, 1749–1758 (2000)
- G. Fibich and B. Ilan. Vectorial and random effects in self-focusing and in multiple filamentation. *Physica D* **157**, 112–146 (2001)
- G. Fibich and B. Ilan. Vectorial effects in self-focusing and multiple filamentation. *Opt. Lett.* **26**, 840–842 (2001)
- G. Fibich and B. Ilan. Multiple filamentation of circularly polarized beams. *Phys. Rev. Lett.* **89**, 013901 (2002)
- G. Fibich and B. Ilan. Self-focusing of circularly polarized beams. *Phys. Rev. E* **67**, 036622 (2003)

- G. Fibich, B. Ilan, and S.V. Tsynkov. Computation of nonlinear backscattering using a high-order numerical method. *Journal of Scientific Computing* **17**, 351–364 (2002)
- G. Fibich, B. Ilan, and S.V. Tsynkov. Backscattering and nonparaxiality arrest collapse of nonlinear waves. *SIAM J. Appl. Math.* **63**, 1718–1736 (2003)
- G. Fibich, V.M. Malkin, and G.C. Papanicolaou. Beam self-focusing in the presence of small normal time dispersion. *Phys. Rev. A* **52**, 4218–4228 (1995)
- G. Fibich and G.C. Papanicolaou. Self-focusing in the perturbed and unperturbed nonlinear Schrödinger equation in critical dimension. *SIAM J. Applied Math.* **60**, 183–240 (1999)
- G. Fibich and G.C. Papanicolaou. Self-focusing in the presence of small time dispersion and nonparaxiality. *Opt. Lett.* **22**, 1379–1381 (1997)
- G. Fibich, W. Ren, and X.P. Wang. Numerical simulations of self focusing of ultrafast laser pulses. *Phys. Rev. E* **67**, 056603 (2003)
- G. Fibich, Y. Sivan, Y. Ehrlich, E. Louzon, M. Fraenkel, S. Eisenmann, Y. Katzir, and A. Zigler. Control of the collapse distance in atmospheric propagation. *Opt. Express* **14**, 4946–4957 (2006)
- G. Fibich and S.V. Tsynkov. High-order two-way artificial boundary conditions for nonlinear wave propagation with backscattering. *J. Comput. Phys.* **171**, 1–46 (2001)
- G. Fibich and S.V. Tsynkov. Numerical solution of the nonlinear Helmholtz equation using nonorthogonal expansions. *J. Comput. Phys.* **210**, 183–224 (2005)
- G.M. Fraiman. Asymptotic stability of manifold of self-similar solutions in self-focusing. *Sov. Phys. JETP* **61**, 228–233 (1985)
- K. Germaschewski, R. Grauer, L. Berge, V.K. Mezentsev, and J.J. Rasmussen. Splittings, coalescence, bunch and snake patterns in the 3D nonlinear Schrödinger equation with anisotropic dispersion. *Physica D* **151**, 175–198 (2001)
- J. W. Grantham, H. M. Gibbs, G. Khitrova, J. F. Valley, and J. J. Xu. Kaleidoscopic spatial instability: Bifurcations of optical transverse solitary waves. *Phys. Rev. Lett.* **66**, 1422–1425 (1991)
- T.D. Grow, A.A. Ishaaya, L.T. Vuong, A.L. Gaeta, N. Gavish, and G. Fibich. Collapse dynamics of super-gaussian beams. *Opt. Express* **14**, 5468–5475 (2006)
- P.L. Kelley. Self-focusing of optical beams. *Phys. Rev. Lett.* **15**, 1005–1008 (1965)
- K. Konno and H. Suzuki. Self-focusing of a laser beam in nonlinear media. *Physica Scripta* **20**, 382–386 (1979)
- I. Kryzhanovskii, B.M. Sedov, V.A. Serebryakov, A.D. Tsvetkov and V.E. Yashin. Formation of the spatial structure of radiation in solid-state laser systems by apodizing and hard apertures. *Sov. J. Quant. Electron.* **13**, 194–198 (1983)
- M.J. Landman, G.C. Papanicolaou, C. Sulem, and P.L. Sulem. Rate of blowup for solutions of the nonlinear Schrödinger equation at critical dimension. *Phys. Rev. A* **38**, 3837–3843, (1988)
- M.J. Landman, G.C. Papanicolaou, C. Sulem, P.L. Sulem and X.P. Wang. Stability of Isotropic Singularities for the Nonlinear Schrödinger Equation. *Physica D* **47**, 393–415, (1991)
- B.J. LeMesurier, G.C. Papanicolaou, C. Sulem, and P.L. Sulem. Local structure of the self-focusing singularity of the nonlinear Schrödinger equation. *Physica D* **32**, 210–226 (1988)
- G.G. Luther, A.C. Newell, and J.V. Moloney. The effects of normal dispersion on collapse events. *Physica D* **74**, 59–73 (1994)
- V.M. Malkin. Dynamics of wave collapse in the critical case. *Phys. Lett. A* **151**, 285–288 (1990)
- V.M. Malkin. On the analytical theory for stationary self-focusing of radiation. *Physica D* **64**, 251–266, (1993)
- J.H. Marburger. Self-focusing: Theory. *Prog. Quant. Electr.* **4**, 35–110 (1975)

- G. Mechain, A. Couairon, M. Franco, B. Prade, and A. Mysyrowicz. Organizing multiple femtosecond filaments in air. *Phys. Rev. Lett.* **93**, 035003 (2004)
- F. Merle. On uniqueness and continuation properties after blow-up time of self-similar solutions of nonlinear Schrödinger equation with critical exponent and critical mass. *Comm. Pure Appl. Math.* **45**, 203–254 (1992)
- F. Merle. Determination of blow-up solutions with minimal mass for nonlinear Schrödinger equation with critical power. *Duke Math. J.* **69**, 427–454, (1993)
- F. Merle and P. Raphael. Sharp upper bound on the blow-up rate for the critical nonlinear Schrödinger equation. *Geom. Funct. Anal.* **13**, 591–642 (2003)
- K.D. Moll, A.L. Gaeta, and G. Fibich. Self-similar optical wave collapse: Observation of the Townes profile. *Phys. Rev. Lett.* **90**, 203902 (2003)
- H. Nawa and M. Tsutsumi. On blow-up for the pseudo-conformally invariant nonlinear Schrödinger equation. *Funkcial. Ekvac.* **32**, 417–428 (1989)
- J.K. Ranka, R.W. Schirmer, and A.L. Gaeta. Observation of pulse splitting in nonlinear dispersive media. *Phys. Rev. Lett.* **77**, 3783–3786 (1996)
- J.E. Rothenberg. Pulse splitting during self-focusing in normally dispersive media. *Opt. Lett.*, **17** 583–585, (1992)
- M. Sever. An existence theorem for some semilinear elliptic systems. *J. Differential equations* **226**, 572–593 (2006)
- Y.R. Shen. Self-focusing: Experimental. *Prog. Quant. Electr.* **4**, 1–34 (1975)
- J.M. Soto-Crespo, E.M. Wright, and N.N. Akhmediev. Recurrence and azimuthal-symmetry breaking of a cylindrical Gaussian beam in a saturable self-focusing medium. *Phys. Rev. A* **45**, 3168–3174 (1992)
- C. Sulem and P.L. Sulem. *The Nonlinear Schrödinger Equation*. Springer, New-York (1999)
- V.I. Talanov. Focusing of light in cubic media. *JETP Lett.* **11**, 199–201 (1970)
- S.N. Vlasov. Structure of the field of wave beams with circular polarization near a nonlinear focus in a cubic medium. *Sov. J. Quantum Electron.* **17**, 1191–1193 (1987)
- S.N. Vlasov, V.A. Petrishchev, and V.I. Talanov. Averaged description of wave beams in linear and nonlinear media. *Izv. Vuz Radiofiz (in Russian)*, **14**, 1353–1363 (1971) *Radiophys. and Quantum Electronics* **14**, 1062–1070 (1971) (in English)
- L.T. Vuong, T.D. Grow, A. Ishaaya, A.L. Gaeta, G.W. Hooft, E.R. Eliel and G. Fibich. Collapse of Optical Vortices. *Phys. Rev. Lett.* **96**, 133901 (2006).
- M.I. Weinstein. Nonlinear Schrödinger equations and sharp interpolation estimates. *Comm. Math. Phys.* **87**, 567–576 (1983)
- N.A. Zharova, A.G. Litvak, T.A. Petrova, A.M. Sergeev, and A.D. Yunakovsky. Multiple fractionation of wave structures in a nonlinear medium. *JETP Lett.*, **44** 13–17 (1986)